EFFECT OF INCORPORATION OF LYSOLIPID ON THE STABILITY OF DIPALMITOYL PHOSPHATIDYL CHOLINE BILAYER MEMBRANE: MOLECULAR DYNAMICS SIMULATION APPROACH

An Undergraduate Thesis
Presented to
The Academic Faculty

by

Keewon Lee

In Partial Fulfillment
of the Requirements for the Bachelor's Degree
in the
School of Biomedical Engineering

Georgia Institute of Technology
May, 2016

EFFECT OF INCORPORATION OF LYSOLIPID ON THE STABILITY OF DIPALMITOYL PHOSPHATIDYL CHOLINE BILAYER MEMBRANE: MOLECULAR DYNAMICS SIMULATION APPROACH

Approved by:

Dr. Seung Soon Jang, Advisor
School of Materials Science and Engineering
Georgia Institute of Technology

Dr. Todd Sulchek
School of Mechanical Engineering
School of Biomedical Engineering
Georgia Institute of Technology

Date Approved:

ACKNOWLEDGEMENTS

I would like to express my full gratitude towards Dr. Seung Soon Jang for his encouragement and support for this precious opportunity. I would also like to thank my undergraduate collaborators: Youngkyung 'Claire' Kim, Hansol Jang, and Heeyoung Yoon for supporting me throughout the research. Lastly, I would like to thank my CNBT lab senior members for providing me with continuous feedback and technical support.

TABLE OF CONTENTS

LIST OF TABLES

LIST OF FIGURES

LIST OF SYMBOLS AND ABBREVIATIONS

DPPC	1, 2-Dipalmitoyl-s n-Glycero-3-Phosphocholine
MPPC	1-Palmitoyl-2-Hydoxy-sn-Glycero-3-Phosphocholine
DPPE	1,2-Bis(diphenylphosphino)ethane
LSTL	Lysolipid Incorporated Thermosensitive Liposomes
MD	Molecular Dynamics
PC	Phosphatidycholine
IFE	Interface Formation Energy

SUMMARY

Previous studies have found that incorporating monopalmitoylphosphatidylcholine(MPPC) lysolipids into PEGylated dipalmitoylphosphatidylcholines(DPPC) membranes of conventional thermosensitive liposomes lowers their phase transition temperature and promote rapid release of the encapsulated drug. Lysolipid has only one acyl chain, arranging the molecule into a conical shape with a relatively large head group compared to its single hydrocarbon tail. In this research, we present a full atomistic molecular dynamic study on the interfacial properties of the lysolipid-incorporated lipid bilayers as a function of structural variable of lipid compositions. We prepared two probable structural configurations of 10% MPPC incorporated DPPC bilayers: a 'dispersed' configuration of which the MPPC lipids are embedded evenly among the DPPC molecules to form a system of lipid layer that have lysolipids evenly distributed over the whole layer, and an 'island' configuration of which a cluster of MPPC lipids is embedded into DPPC molecules forming a island of lysolipid-agglomerate in the bilayer. Using two configurations, we analyzed how the intermolecular configuration of lysolipid-incorporated lipid bilayer affects the macroscopic properties of the bilayer between the water phases. For this purpose, the energetic profiles, density profile, and the structural correlations of the molecules where characterized for both configurations of 'island' and 'dispersed' system. The results indicate that the island system may be a promising structure for composing 10% MPPC incorporated DPPC bilayers. This study not only determines the probable structural composition of mixed MPPC/DPPC lipid bilayer but also

better understands the role of the lysolipids affecting the overall behavior of the lipid bilayer.

CHAPTER 1

INTRODUCTION

Phosphatidycholines (PC) are phospholipids composed of choline headgroup and glycerophosphoric acids. Due to concurrence of both lipophilic and hydrophilic components, PCs are amphiphiles that spontaneously assemble themselves into bilayers in aqueous environment, positioning hydrophilic heads towards the surrounding aqueous medium and their lipophilic alkyl chains towards the inside of the bilayer, creating a non-polar region between two polar regions.

Among several classes of PCs, dipalmitoylphosphatidylcholines (DPPC) are one of the most commonly studied PCs for their ability to transform their formation of bilayer film into spherical vesicles [1][2]. These vesicles, also termed liposomes, have emerged as promising drug carriers that can retain the drug, evade the body's defense system during circulation, and target the pathogenic tissue passively or specifically [2]. One of the biggest challenges in the liposomal design is to initiate and control the release of the drug from the carriers once they have reached the targeted site. Temperature-sensitive liposomes [3][4] have been proposed to achieve this systemic functionality, but still faced limitations in increasing the efficiency of the drug release at clinically attainable temperature in the range of 39 to 41C.

In this paper, we present a full atomistic molecular dynamic study on the interfacial properties of the lysolipid-incorporated lipid bilayers as a function of structural variable of lipid compositions. We prepared two probable structural configurations of 10% MPPC incorporated DPPC bilayers: a 'dispersed' configuration of which the MPPC lipids are embedded evenly among the DPPC molecules to form a system of lipid layer

that have lysolipids evenly distributed over the whole layer (Figure 2), and an 'island' configuration of which a cluster of MPPC lipids is embedded into DPPC molecules forming a island of lysolipid-agglomerate in the bilayer (Figure 2). Using two configurations, our aim is to analyze how the intermolecular configuration of lysolipid-incorporated lipid bilayer affects the macroscopic properties of the bilayer between the water phases. For this purpose, the energetic profiles, density profile, and the structural correlations of the molecules where characterized for both configurations of 'island' and 'dispersed' system. This study not only provides better understanding in determining probable conformation of LSTL bilayers but also reveal macroscopic properties of the bilayer affected by the incorporation of lysolipid at molecular level.

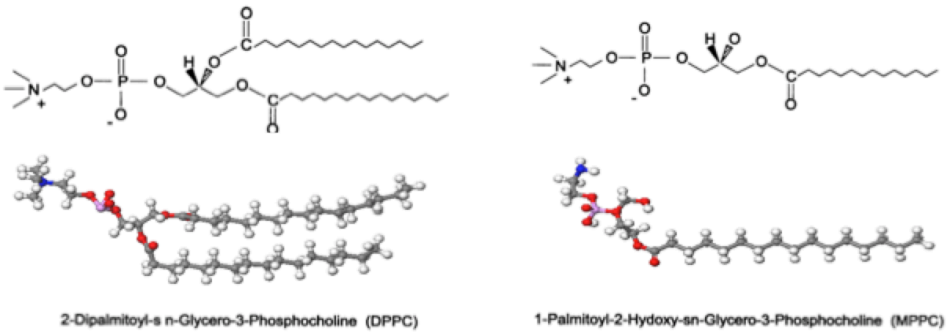

Figure 1. Configuration of DPPC (left) and MPPC (right) molecules used in the simulation.

CHAPTER 2

LITERATURE REVIEW

In 1999, Needham and his co-workers first proposed the idea of incorporating monopalmitoylphosphatidylcholine (MPPC) lysolipids into PEGylated DPPC membranes of conventional thermosensitive liposomes in order to lower the phase transition and promote rapid drug release [5]. Lysolipid has only one acyl chain, providing the lipid a conical molecular shape accompanied by a relatively large head group compared to its single hydrocarbon tail. Previous studies have shown that the incorporation of MPPC to the DPPC liposome in 10 mol % lowers the phase transition temperature from 43C to 39-40C, increasing the release rate of the encapsulated drug by 70%[6][7]. Subsequently, studies on human xenograft models have demonstrated that lysolipid incorporated thermosensitive liposomes (LSTL), when applied with mild hyperthermia, are more effective in reducing tumor growth than free drugs, traditional thermosensitive liposomes, and non-thermosensitive liposomes [6][7][8].

Despite of its promising chemotherapeutic features, the attempts to understand the mechanism of LSTL have been facing difficulties. Mass spectrometry analysis showed that the lysolipids remained in the membranes after dialysis above the phase transitional temperature indicating possibility of lysolipid-stabilized pores for the mechanism of rapid drug release [9]. Coarse-grained molecular dynamic simulations of LSTL bilayer showed that the peak permeability coincided with the phase transition from the gel to liquid-crystalline state when there was sharp jump in area per lipid while lysolipid MPPCs were present, supporting the possibility of lysolipid-stabilized pores as the reason for the enhanced permeability of the LSTL [10][11]. However, current study have revealed that

the lysolipids desorbed from the LSTL bilayer at 37C, and more than half of the lysolipids have been detached from the LSTL in vivo within 1hour after injection, reducing the temperature sensitivity of the LSTL [12]. Another study has shown that LSTLs that still had lysolipids had lost their permeability by 50% in vitro, questioning the functionality of lysolipids on the lipid bilayer. [13] More confusingly, LSTL in serum containing media had drug leakage at 37C, which is lower than the transitional temperature.

Molecular modeling approaches such as the molecular dynamics (MD) and Monte Carlo (MC) simulations have been extensively used for studying lipid bilayer of mixed lipid components [14][15][16][17][18][19]. The lipid-cholesterol mixtures are predicted to exhibit solid phase immiscibility at low temperatures causing cholesterols to localize in the membrane [17][18][19]. Similarly, the DPPE molecules in mixed DPPE/DPPC bilayers were shown to move laterally and exhibit more localized movement under increasing concentrations [16]. These localized DPPE molecules determined the behavior of the total bilayer due to their competitive interactions with water molecules or the phosphate groups of DPPC molecules. However, none of the simulations so far has studied the behavior of DPPC layers that contains lysolipid on atomistic/molecular level.

CHAPTER 3

MODEL AND SIMULATION PREPARATION

All simulations were carried out using full-atomistic models of 10 mol% of MPPC incorporated DPPC bilayer with water content. The compositions of the 'Dispersed' and 'Island' systems are summarized in Table 1.

TABLE 1 : Components of 'Dispersed' and 'Island' System

	'Dispersed' and 'Island' system		
	DPPC	MPPC	H_2O
# of molecules	108	12	6920

Force Field and Simulation Parameters

For this study, MPPC and DPPC molecules were described using Dreiding force field developed by Mayo and his co-workers [20], and water molecules using F3C model [21]. These force fields were consistently tested and successfully implemented in molecular dynamic simulations in the previous studies on self assembled interfaces [22][23][24][25][26][27][28][29][30][31], and biological models [32][33]. The total potential energy is given as follows:

$$E_{total} = E_{vdW} + E_Q + E_{bond} + E_{angle} + E_{torsion}$$

where E_{total}, E_{vdW}, E_Q, E_{bond}, E_{angle}, and $E_{torsion}$ are the total energy and the van der Waals, electrostatic, bond-stretching, angle-bending, and torsion-energy components, respectively. The individual atomic charges were assigned through the Mulliken population analysis using B3LYP and 6-31G** in Jaguar [34]. The Particle-Particle

Particle-Mesh (PPPM) method [35][36] was used to calculate the long-range electrostatic interactions.

Throughout this research, all MD simulations were performed with the LAMMPS [37][38] (large-scale atomic/molecular massively parallel simulator) from Sandia National Laboratories modified to handle our force fields [22]. The equations of motion were integrated using Verlet algorithm [39] with a time step of 1.0 fs. A Nose-Hoover thermostat [40][41] with relaxation time of 0.1 ps was used to achieve constant temperature conditions for both NVT and NPT MD simulations. Pressure was controlled isotropically. The standard geometric combination rules for Lennard-Jones potentials were used for the interactions between heterogeneous atomic pairs (water and the lipids).

Model and MD Simulation

The chemical structures of water, DPPC, and MPPC models used in the simulation are shown in Figure 1. Both 'dispersed' and 'island' systems were simulated in presence of water phases on both sides of the lipid bilayer, which have been widely used for the studies of lipid bilayers [cite]. Both systems contain 120 lipids (12 MPPC and 108 DPPC) arranged as corresponding bilayer configurations with 6920 water molecules distributed on top and bottom of the bilayer Figure 2. When constructing either the 'dispersed' or the 'island' bilayer, the MPPC and the DPPC molecules in 1:10 ratio were packed into most suitable hexagonally closest structure in an orthorhombic simulation box with periodic boundary condition applied for all spatial directions Figure 2. Then energy minimization was carried out to relax the constructed bilayer with fixed L_x, L_y, and L_z directions. Next, we prepared water phases separately using NVT MD simulations based on the experimental densities of 0.997 g/cm^3 at 300K. We then

integrated the prepared water phases into the prepared simulation box containing either 'dispersed' or 'island' lipid bilayer. For both hydrated 'dispersed' and 'island' cell boxes, energy minimization was again carried out to prepare the initial systems in which the interaction between the water and the lipid phases are adjusted. Once the initial systems for both configurations were prepared, NVT and NPT MD simulations were sequentially carried out to equilibrate the systems. First, a NVT MD simulation was performed for 400 ps at 300K as a pretreatment for overcoming local minima by imposing thermal energy in a constant volume condition. A final equilibration was done for both systems by a NPT MD simulation for 5ns at 300K and 1 atm to adjust the system to a more realistic density. Table 2 indicates the equilibrated cell parameters of the simulation box for both 'dispersed' and 'island' system at 300K. All the modeling and energy minimization jobs in this work were done through Cerius^2 platform [42] from Accelrys, Inc.

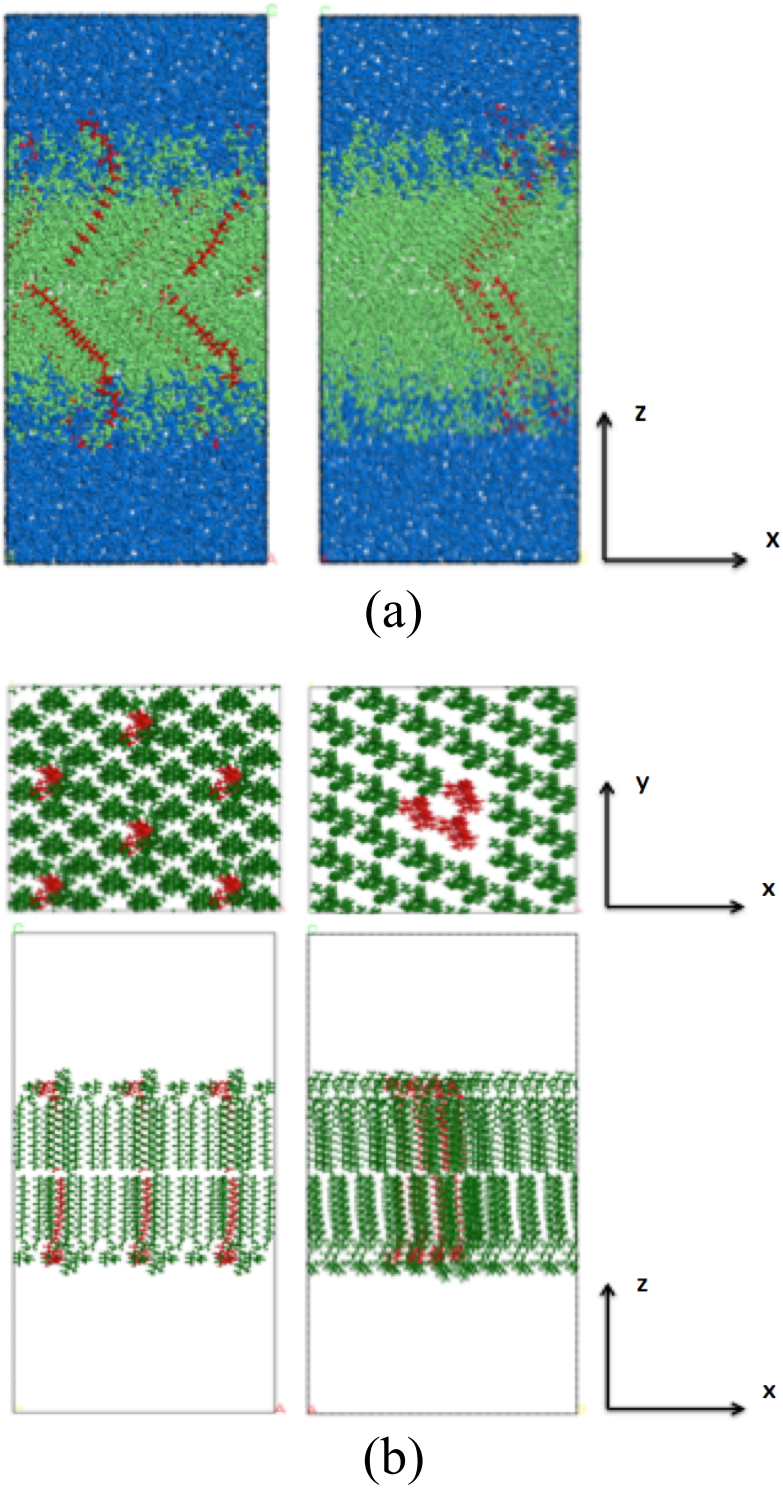

Figure 2. (a) Simulated configuration of 'dispersed' (left) and 'island' (right) system. The water molecules, DPPCs, and MPPCs are shown blue, green, and red, respectively. (b) The initial hexagonal packing of 'dispersed' and 'island' structure of MPPC incorporated Lipid bilayer. MPPC and DPPC are shown red and green, respectively.

CHAPTER 4

RESULTS

Equilibrated System : Interfacial Area and Interfacial Formation Energy

Figure 2a illustrates snapshot of the equilibrated structure of 'dispersed' and 'island' system after 5ns equilibrium. The volumetric properties for both systems were converged from the equilibrium since the volume fluctuation from a subsequent 1ns NPT MD simulation for data collection is less than 1% of the average value. The fluctuations of the cell in each dimension for both configurations are summarized in Table 2. The interfacial area (L_x x L_y) of the 'dispersed' configuration is slightly larger than the 'island' system by 0.1%.

Interface formation energy (IFE) is a measure of the averaged intermolecular interaction per lipid molecule arising from the formation of lipid bilayer in water phase. The energetic stability between the 'dispersed' and 'island' system was compared via IFE defined as follows:

$$IFE = \frac{\left(E_{total} - \left(n \times E_{lipid,single} + E_{water}\right)\right)}{n}$$

where E_{total} reperesents the energies of the whole system, $E_{lipid,single}$ represents the single lipid molecule that is calculated from separate 2ns MD simulation in vacuum at the sample temperature, and E_{water} represents the energy of bulk water phase from a separate 1ns MD simulation of a water box with the same number of water molecules used in the total system at the same temperature. The components necessary for this calculation and the results are summarized in Table 3. The 'island' configuration had lower E_{total} and

thereby the lower IFE than that of 'dispersed' configuration for both 300K and 305K simulations.

TABLE 2 : Equilibrated Cell Parameters of the Simulation Box at 300K and 305K

System		*Lx* (Å)	*Ly* (Å)	*Lz* (Å)	Area/molecule(Å^2)
300K	Dispersed	67.86 ± 0.21	50.22 ± 0.31	102.76 ± 0.54	56.80 ± 0.53
	Island	62.09 ± 0.35	54.39 ± 0.34	103.76 ± 0.82	56.28 ± 0.67
305K	Dispersed	68.21 ± 0.12	49.52 ± 0.53	103.78 ± 0.76	56.30 ± 0.18
	Island	61.53 ± 0.43	55.13 ± 0.12	103.51 ± 0.45	56.53 ± 0.28

TABLE 3 : Interface Formation Energy

	System	E_{total} (kcal/mol)	E_{dppc} (kcal/mol)	E_{mppc} (kcal/mol)	E_{water} (kcal)	IFE (kcal/mol)
300K	Dispersed	-65605 ± 182	172 ± 8.53	120 ± 7.24	-69434 ± 152	-135 ± 5.61
	Island	-65681 ± 173	172.12 ± 8.53	120 ± 7.24	-69434 ± 152	-136 ± 5.69
305K	Dispersed	-64842 ± 176	169 ± 11.0	124 ± 8.36	-68812 ± 146	-131 ± 10.99
	Island	64801 ± 184	169 ± 11.0	124 ± 8.36	-68812 ± 146	-131 ± 11.05

Density Profiles

Figure 3 and 4 shows the density profiles of each system along the z-axis direction of the simulation box, which were obtained by dividing the system into 1.5 Å thick slabs parallel to the xy plane. In each density profile, the distribution of the water, DPPC, MPPC molecules, as well as the distribution of the nitrogen and phosphorous atoms in the choline and phosphate groups of the lipids are illustrated. It is clear that the system consists of two phases that yield invariant density and two well-defined interfaces that can be defined by varying density.

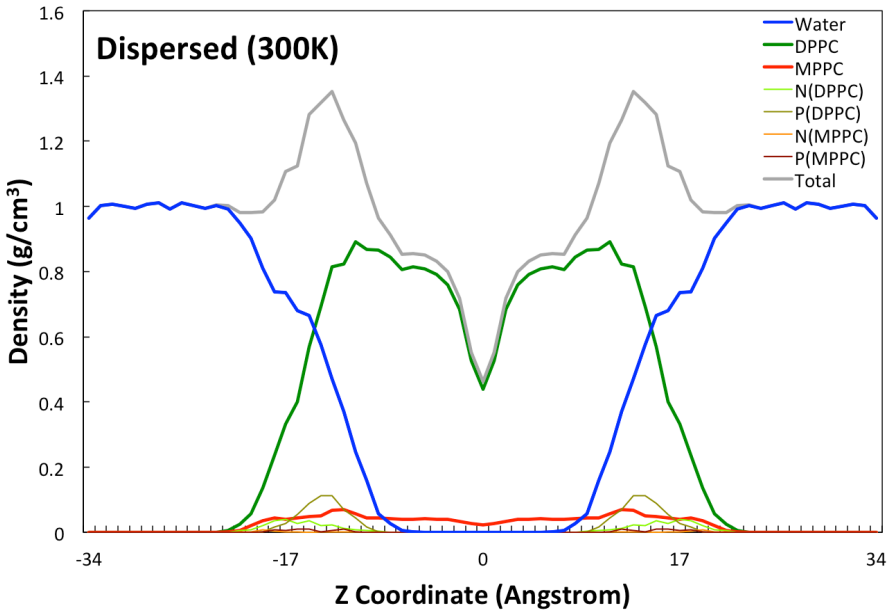

(a)

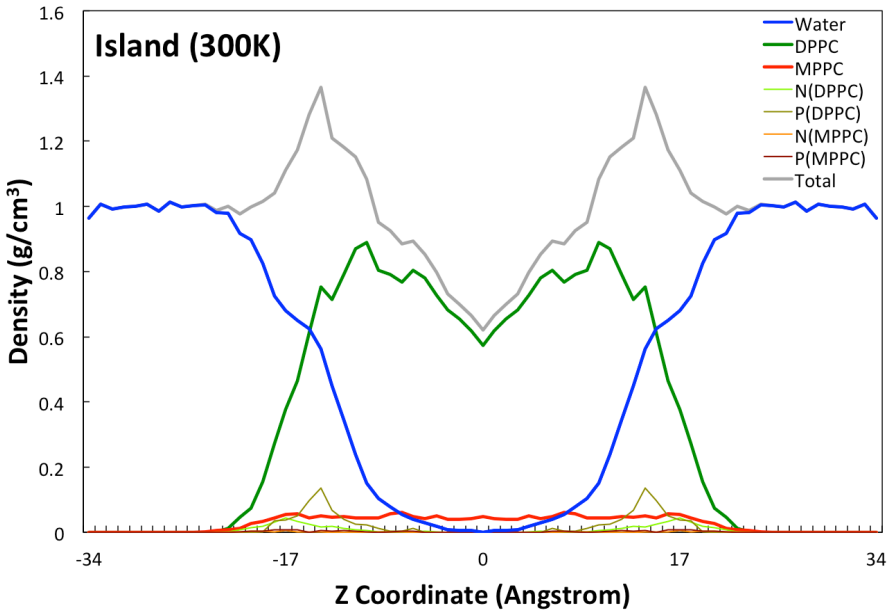

(b)

Figure 3. Density profiles along the z-axis direction of 'dispersed' and 'island' system at 300K.

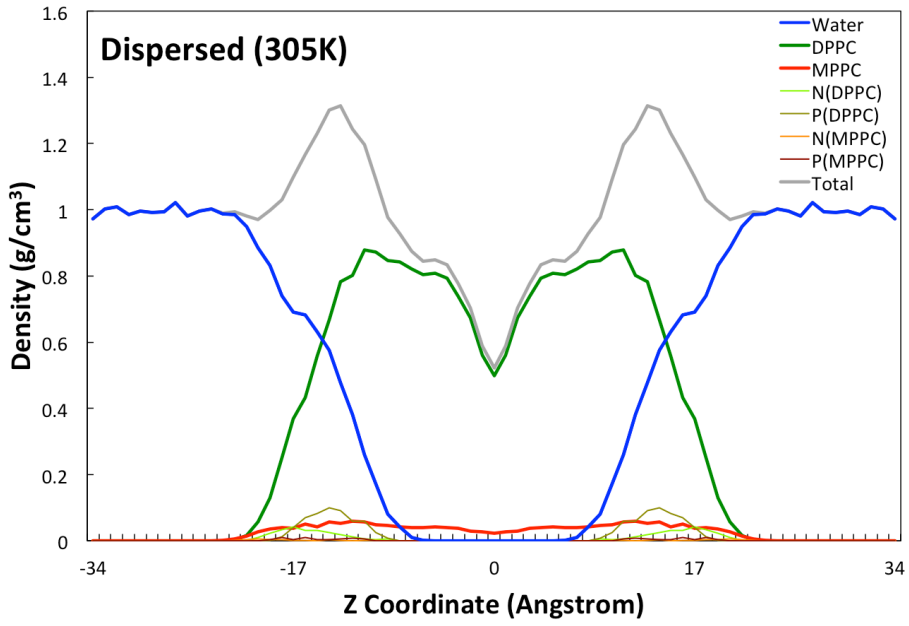

(a)

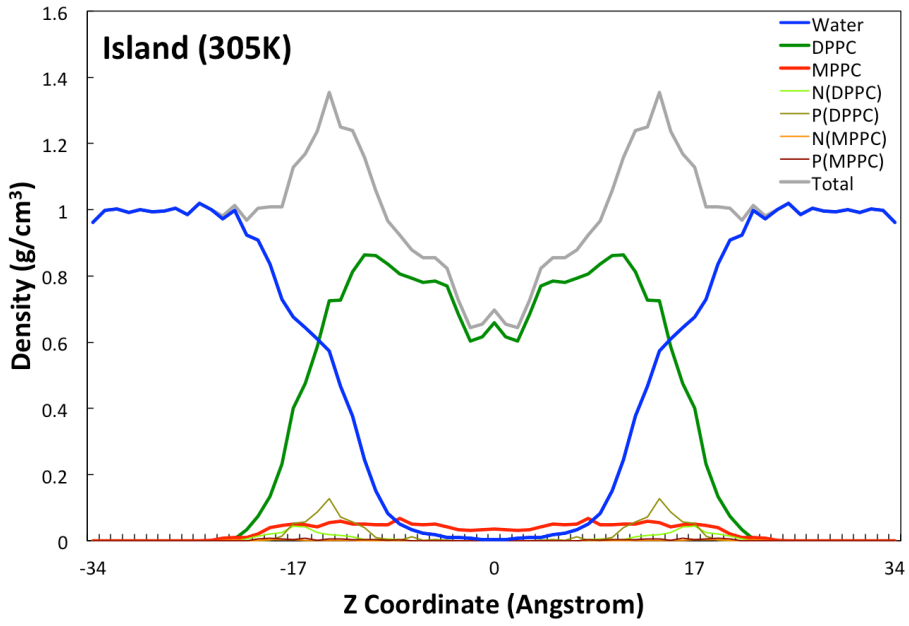

(b)

Figure 4. Density profiles along the z-axis direction of 'dispersed' and 'island' system at 305K.

Pair Correlation Functions

In order to understand the internal distribution of water, DPPC, and MPPC molecules and their spatial relationship between each other, we represented the pair correlation between choline groups of DPPC and the choline groups of MPPC, the correlation between choline groups of both lipids and the water molecules, and the correlation between the phosphate groups of both lipids and the water molecules. This would allow us to better investigate the interactions of water molecules with the DPPC and MPPC molecules at the interface in both 'dispersed' and 'island' systems. The pair correlation is represented by the radial distribution function below:

$$g_{A-B}(r) = \left(\frac{n_B}{4\pi^2 \Delta r}\right) / \left(\frac{N_B}{V}\right)$$

where n_B is the number of atoms B located at the distance r in a shell of thickness r from atom A, N_B is the number of B particles in the system, and V is the total volume of the system.

Figure 5 and 6 illustrate the distinguishable spatial distribution of MPPC between the two configurations. From Figure 5, $\rho g_{N(MPPC)\text{-}N(MPPC)}(r)$ of the dispersed system simulated in both 300K and 305K shows no signal at the distance closer than 14 Å, which is simply due to the far distance among the MPPCs whereas $\rho g_{N(MPPC)\text{-}N(MPPC)}(r)$ of the island system has two characteristic peaks at the distance closer than 14 Å. From this result, we are able to estimate the averaged distance among the MPPCs in the lipid bilayer. From Figure 6, $\rho g_{N(MPPC)\text{-}N(DPPC)}(r)$ of island system in both 300K and 305K has lower intensity than that of the dispersed system. This is an expected result from MPPCs in the island system aggregating together to form a domain in the bilayer. In contrast,

MPPCs in the dispersed system are dispersed through the bilayer and surrounded by the neighboring DPPCs.

Figure 7 and 8 illustrates the difference in the spatial distribution of water and the polar head groups of between MPPC and DPPC in both lipid bilayer configurations under 300K and 305K simulations. For both system, $\rho g_{N(DPPC)\text{-}O(water)}(r)$ and $\rho g_{N(MPPC)\text{-}O(water)}(r)$ have similar positions for the peaks. The intensity of $\rho g_{N(MPPC)\text{-}O(water)}(r)$ for the dispersed system is slightly higher than that of $\rho g_{N(DPPC)\text{-}O(water)}(r)$. For the island system, the intensity of $\rho g_{N(MPPC)\text{-}O(water)}(r)$ is nearly similar with that of $\rho g_{N(DPPC)\text{-}O(water)}(r)$.

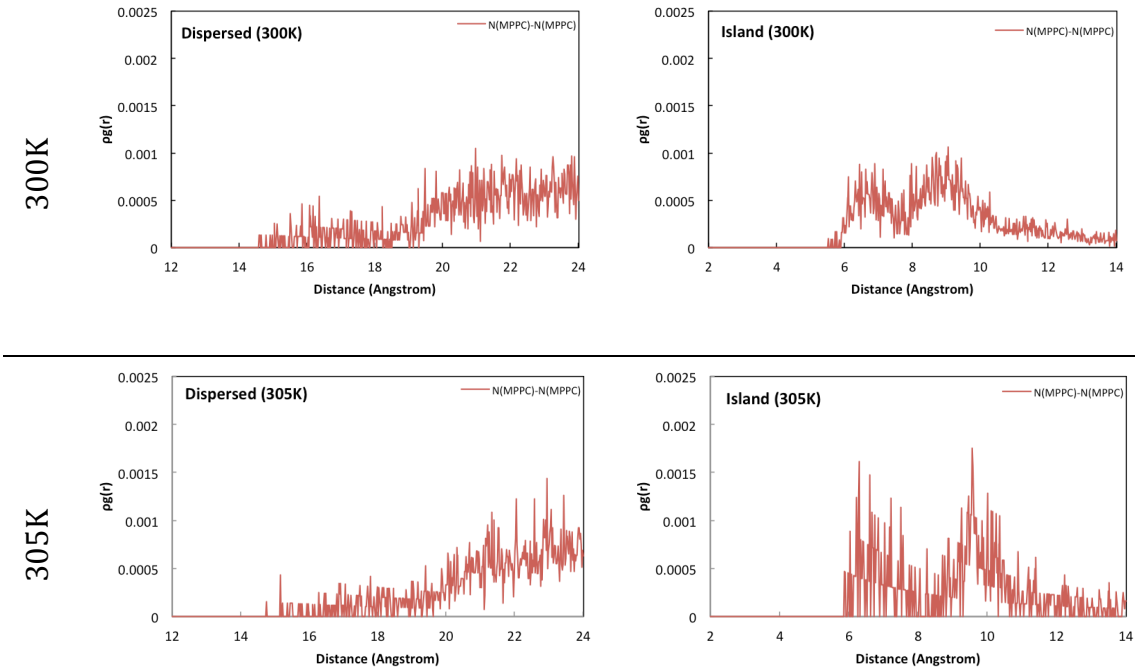

Figure 5. Pair correlation function of nitrogen-nitrogen on MPPC molecules, $\rho g_{N(MPPC)\text{-}N(MPPC)}(r)$, in 'dispersed' and 'island' system for 300K and 305 simulations.

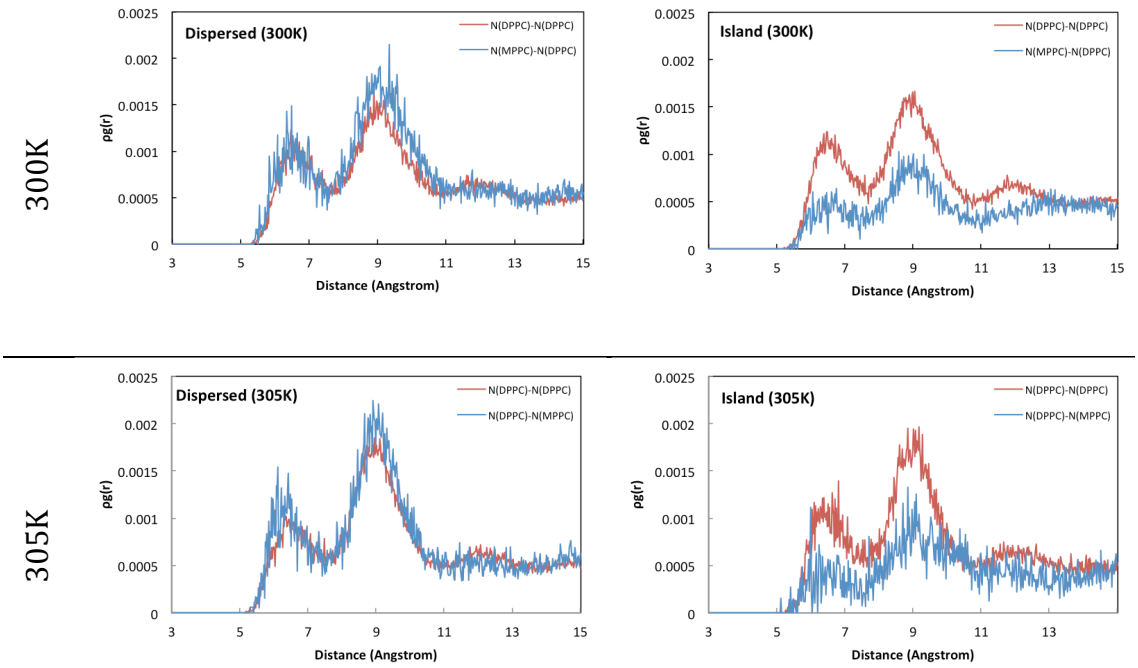

Figure 6 Pair correlation function of nitrogen-nitrogen on DPPC molecules, $\rho g_{N(DPPC)-N(DPPC)}(r)$, nitrogen-nitrogen on MPPC molecules, $\rho g_{N(MPPC)-N(MPPC)}(r)$, in 'dispersed' and 'island' system for 300K and 305K simulations.

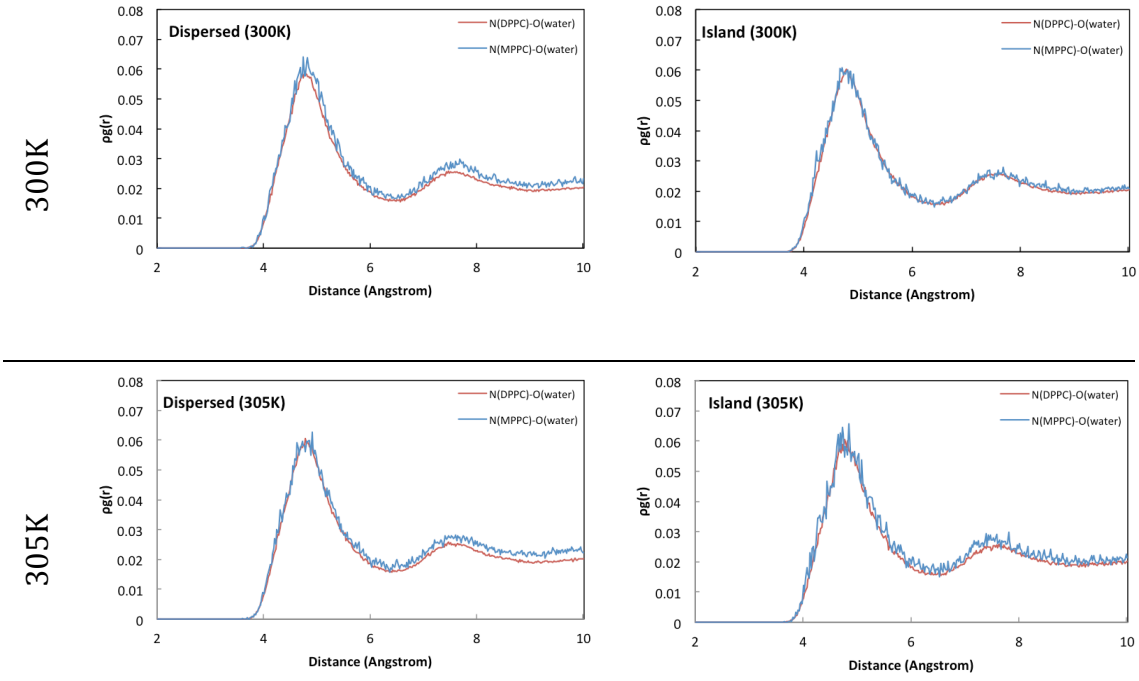

Figure 7. Pair correlation function of nitrogen on DPPC and oxygen on water molecules, $\rho g_{N(DPPC)\text{-}O(water)}(r)$, nitrogen on MPPC and oxygen on water $\rho g_{N(MPPC)\text{-}O(water)}(r)$, in 'dispersed' and 'island' system for 300K and 305K simulations.

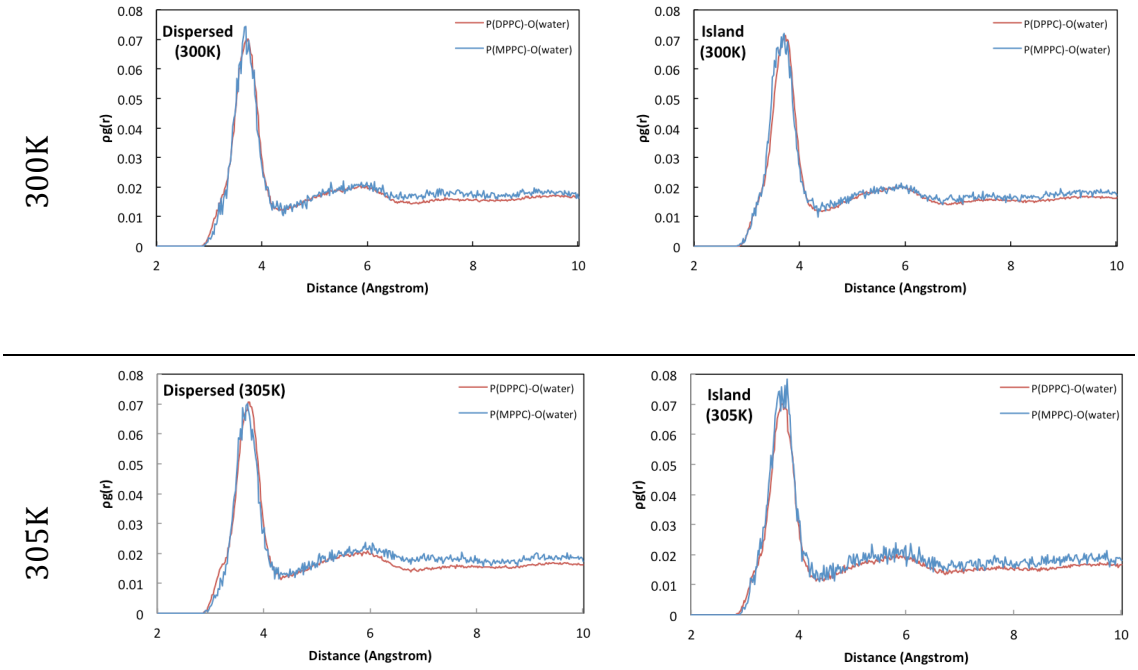

Figure 8. Pair correlation function of phosphorous on DPPC and oxygen on water molecules, $\rho g_{P(DPPC)\text{-}O(water)}(r)$, phosphorous on MPPC and oxygen on water molecules, $\rho g_{N(DPPC)\text{-}O(water)}(r)$, in 'dispersed' and 'island' system for 300K and 305K simulations.

CHAPTER 5

DISCUSSIONS

Energy Profiles of the Equilibrated System

The 'island' configuration had lower E_{total} and thereby the lower IFE than that of the 'dispersed' configuration for both 300K and 305K simulations, implying that the 'island' configuration of the LSTL bilayer could be energetically favorable. This result raises possible indication that the 'dispersed' system, where individual MPPCs are evenly embedded throughout the DPPC bilayer, may not be a stable structure when composing 10% MPPC LSTL. However, further simulations are needed to confirm this energetic profile. It would be interesting to see if this trend continues throughout the transitional temperature of 313.5K, when the bilayers are expected to turn into liquid crystalline phase from the gel phase.

Internal Structural Configurations of the Lipid Layers

From the density profile (Figure 3 and 4), it is clear that both 'dispersed' and 'island' system consist of two phases that yield invariant density and two well-defined interfaces that can be defined by the varying density. Another noteworthy feature in both 300K and 305K simulations is that most phosphorous and nitrogen ions stay between the water and the lipid monolayer in both 'dispersed' and 'island' configurations. The distribution of water molecules within the choline and phosphorous groups are well characterized within this theme. The significant density difference between the 'dispersed' and 'island' configuration occurs at the center of the slab, which is the middle of the lipid bilayer. Compared to the 'dispersed' system, the densities of DPPC and MPPC lipids of the 'island' system are higher within the bilayer where the water

molecules have not diffused through. This indicates that the lipids in 'island' system are tended to have more compact interactions between the two layers compared to the lipids in the 'dispersed' system. These stronger interactions between the lipids could be a possible factor affording the formation of stable interface between the water phases for the 'island' configuration. This trend is more significant according to increasing temperature, as shown in the density distribution of the systems during 305K simulations. Both MPPC and DPPC lipids in the 'island' configuration are increasingly proportioned through at the center of the lipid bilayer.

MPPC Lipids and Water Interactions

For both dispersed and island system, $\rho g_{N(DPPC)\text{-}O(water)}(r)$ and $\rho g_{N(MPPC)\text{-}O(water)}(r)$ have similar positions for the peaks (Figure 7). However, it is significant that the intensity of $\rho g_{N(MPPC)\text{-}O(water)}(r)$ for the dispersed system is slightly higher than that of $\rho g_{N(DPPC)\text{-}O(water)}(r)$. For the island system, the intensity of $\rho g_{N(MPPC)\text{-}O(water)}(r)$ is nearly similar with that of $\rho g_{N(DPPC)\text{-}O(water)}(r)$. This difference in intensity may indicate that the MPPC in the dispersed system is solvated by water more. Since individual MPPC molecules are embedded throughout the DPPC lipid layer in the dispersed configuration, it is possible that the MPPCs are not packed fully inside the layer due to their insufficient interactions with the DPPC tails. Consequently, the polar head groups of the MPPC molecules would protrude from the layer, allowing higher interactions with the water molecules. This trend is not shown in the island configurations because the MPPC molecules are fully embedded in the DPPC layers as a packed cluster. Similar results was shown from the intensities of the $\rho g_{P(DPPC)\text{-}O(water)}(r)$ and $\rho g_{P(MPPC)\text{-}O(water)}(r)$ where the phosphorous of the MPPC headgroups have higher density correlation with the water molecules in the

dispersed configuration system to those of the island system (Figure 8). However, further investigation on the relationship between the MPPC headgroups and the water is needed in increasing temperature to confirm this difference in lipid interaction properties occurring at the water and lipid interface.

CHAPTER 6

CONCLUSION AND FUTURE PLANS

Based on the result of MD simulation in 300K and 305K, lysolipid-incorporated lipid bilayer of ‘island’ configuration is resulted to be energetically stable as that of ‘dispersed’ configuration. The internal lipid distribution, interfacial thickness and the choline-phosphate conformity seemed to differ between two configurations, and the water molecules are more correlated to the headgroups of the lysolipids in ‘dispersed’ system compared those of the ‘island’ system. This may be an indication of lysolipids detaching from the bilayer, but the data is not enough to support this consequence. Further analysis such as the difference between the mean square displacement between the DPPC and MPPC, and the coordination number between nitrogen of lipids and the oxygen of water should be calculated. Furthermore, analysis from simulations in higher temperature setup (310K, 315K and 320K) should be consolidated to come up with a more confined solution in explaining the behavior of this lysolipid incorporated lipid bilayer in aqueous environment.

REFERENCES

[1] Alex H. de Vries , A. E. M., and Siewert J. Marrink, Molecular Dynamics Simulation of the Spontaneous Formation of a Small DPPC Vesicle in Water in Atomistic Detail. J. Am. Chem. Soc 2004, 126 (14), 4488–4489.

[2] Allen, T. M., Liposomes - Opportunities in drug delivery. Drugs 1997, 54, 8-14.

[3] Ta, T.; Porter, T. M., Thermosensitive liposomes for localized delivery and triggered release of chemotherapy. J Control Release 2013, 169 (1-2), 112-125.

[4] Yatvin, M. B.; Weinstein, J. N.; Dennis, W. H.; Blumenthal, R., Design of liposomes for enhanced local release of drugs by hyperthermia. Science 1978, 202 (4374), 1290-3.

[5] Anyarambhatla, G. R.; Needham, D., Enhancement of the phase transition permeability of DPPC liposomes by incorporation of MPPC: A new temperature-sensitive liposome for use with mild hyperthermia. Journal of liposome research 1999, 9 (4), 491-506.

[6] Kong, G.; Anyarambhatla, G.; Petros, W. P.; Braun, R. D.; Colvin, O. M.; Needham, D.; Dewhirst, M. W., Efficacy of liposomes and hyperthermia in a human tumor xenograft model: Importance of triggered drug release. Cancer Res 2000, 60 (24), 6950-6957.

[7] Needham, D.; Anyarambhatla, G.; Kong, G.; Dewhirst, M. W., A new temperature-sensitive liposome for use with mild hyperthermia: Characterization and testing in a human tumor xenograft model. Cancer Res 2000, 60 (5), 1197-1201.

[8] Mills, J. K.; Eichenbaum, G.; Needham, D., Effect of bilayer cholesterol and surface grafted poly(ethylene glycol) on pH-induced release of contents from liposomes by poly(2-ethylacrylic acid). Journal of liposome research 1999, 9 (2), 275-290.

[9] Mills, J. K.; Needham, D., Lysolipid incorporation in dipalmitoylphosphatidylcholine bilayer membranes enhances the ion permeability and drug release rates at the membrane phase transition. Biochim Biophys Acta 2005, 1716 (2), 77-96.

[10] Winter, N. D.; Schatz, G. C., Coarse-Grained Molecular Dynamics Study of Permeability Enhancement in DPPC Bilayers by Incorporation of Lysolipid. Journal of Physical Chemistry B 2010, 114 (15), 5053-5060.

[11] Winter, N. D.; Murphy, R. K. J.; O'Halloran, T. V.; Schatz, G. C., Development and modeling of arsenic-trioxide--loaded thermosensitive liposomes for anticancer drug delivery. Journal of liposome research 2011, 21 (2), 106-115.

[12] Banno, B.; Ickenstein, L. M.; Chiu, G. N. C.; Bally, M. B.; Thewalt, J.; Brief, E.; Wasan, E. K., The Functional Roles of Poly(Ethylene Glycol)-Lipid and Lysolipid in the Drug Retention and Release from Lysolipid-Containing Thermosensitive Liposomes In Vitro and In Vivo. J Pharm Sci-Us 2010, 99 (5), 2295-2308.

[13] Sandstrom, M. C.; Ickenstein, L. M.; Mayer, L. D.; Edwards, K., Effects of lipid segregation and lysolipid dissociation on drug release from thermosensitive liposomes. J Control Release 2005, 107 (1), 131-142.

[14] Khelashvili, G. A.; Scott, H. L., Combined Monte Carlo and molecular dynamics simulation of hydrated 18:0 sphingomyelin-cholesterol lipid bilayers. J Chem Phys 2004, 120 (20), 9841-7.

[15] Michonova-Alexova, E. I.; Sugar, I. P., Component and state separation in DMPC/DSPC lipid bilayers: a Monte Carlo simulation study. Biophys J 2002, 83 (4), 1820-33.

[16] Leekumjorn, S.; Sum, A. K., Molecular simulation study of structural and dynamic properties of mixed DPPC/DPPE bilayers. Biophys J 2006, 90 (11), 3951-65.

[17] Scott, H. L., Lipid-cholesterol interactions. Monte Carlo simulations and theory. Biophys J 1991, 59 (2), 445-55.

[18] Saito, H.; Shinoda, W., Cholesterol effect on water permeability through DPPC and PSM lipid bilayers: a molecular dynamics study. The journal of physical chemistry. B 2011, 115 (51), 15241-50.

[19] Sabatini, K.; Mattila, J. P.; Kinnunen, P. K., Interfacial behavior of cholesterol, ergosterol, and lanosterol in mixtures with DPPC and DMPC. Biophys J 2008, 95 (5), 2340-55.

[20] Mayo, S. L.; Olafson, B. D.; Goddard, W. A., III Dreiding - a Generic Force-Field for Molecular Simulations. J. Phys. Chem. 1990, 94, 8897−8909.

[21] Levitt, M.; Hirshberg, M.; Sharon, R.; Laidig, K. E.; Daggett, V., Calibration and testing of a water model for simulation of the molecular dynamics of proteins and nucleic acids in solution. *Journal of Physical Chemistry B* **1997,** *101* (25), 5051-5061.

[22] Jang, S. S.; Lin, S.-T.; Maiti, P. K.; Blanco, M.; Goddard, W. A., III; Shuler, P.; Tang, Y. Molecular Dynamics Study of Surfactant- Mediated Decane/Water Interface: Effect of Molecular Architecture of Alkyl Benzne Sulfonate. J. Phys. Chem. B 2004, 108, 12130−12140.

[23] Jang, S. S.; Goddard, W. A., III Structures and Properties of Newton Black Films Characterized Using Molecular Dynamics Simulations. J. Phys. Chem. B 2006, 110, 7992−8001.

[24] Jang, S. S.; Jang, Y. H.; Kim, Y.-H.; Goddard, W. A., III; Choi, J. W.; Heath, J. R.; Laursen, B. W.; Flood, A. H.; Stoddart, J. F.; Norgaard, K.; et al. Molecular Dynamics Simulation of Amphiphilic Bistable [2] Rotaxane Langmuir Monolayer at the Air/Water Interface. J. Am. Chem. Soc. 2005, 127, 14804−14816.

[25] Jang, S. S.; Jang, Y. H.; Kim, Y.-H.; Goddard, W. A., III; Flood, A. H.; Laursen, B. W.; Tseng, H.-R.; Stoddart, J. F.; Jeppesen, J. O.; Choi, J. W.; et al. Structures and Properties of Self-Assembled Monolayers of Bistable [2]Rotaxanes on Au (111) Surfaces from Molecular Dynamics Simulations Validated with Experiment. J. Am. Chem. Soc. 2005, 127, 1563−1575.

[26] Kim, Y. H.; Jang, S. S.; Goddard, W. A., III Possible Performance Improvement in [2]Catenane Molecular Electronic Switches. Appl. Phys. Lett. 2006, 88, 163112.

[27] Kim, Y. H.; Jang, S. S.; Goddard, W. A., III Conformations and Charge Transport Characteristics of Biphenyldithiol Self-Assembled- Monolayer Molecular Electronic Devices: A Multiscale Computational Study. J. Chem. Phys. 2005, 122, 244703.

[28] Kim, Y. H.; Jang, S. S.; Goddard, W. A., III Conformations and Charge Transport Characteristics of Biphenyldithiol Self-Assembled- Monolayer Molecular Electronic Devices: A Multiscale Computational Study (Vol 122, Art No 244703, 2005). J. Chem. Phys. 2005, 123, 169902.

[29] Kim, Y. H.; Jang, S. S.; Jang, Y. H.; Goddard, W. A., III First- Principles Study of the Switching Mechanism of 2 Catenane Molecular Electronic Devices. Phys. Rev. Lett. 2005, 94, 156801.

[30] George, C.; Yoshida, H.; Goddard, W. A., III; Jang, S. S.; Kim, Y. H. Charge Transport through Polyene Self-Assembled Monolayers from Multiscale Computer Simulations. J. Phys. Chem. B 2008, 112, 14888−14897.

[31] Kim, H.; Jang, S. S.; Kiehl, R. A.; Goddard, W. A., III Negative Differential Resistance of Oligo(Phenylene Ethynylene) Self- Assembled Monolayer Systems: The Electric-Field-Induced Con- formational Change Mechanism. J. Phys. Chem. C 2011, 115, 3722− 3730.

[32] Choi, E. J.; Mao, J.; Mayo, S. L., Computational design and biochemical characterization of maize nonspecific lipid transfer protein variants for biosensor applications. *Protein Sci* **2007,** *16* (4), 582-588;

[33] Raghuvir R.S. Pissurlenkar, M. S. S., Radhakrishnan P. Iyer, and Evans C. Coutinh, Molecular Mechanics Force Fields and their Applications in Drug Design. *Anti-Infective Agents in Medicinal Chemistry* **2009,** *8*, 128-150.

[34] Jaguar, 7.5; Schrödinger, LLC: New York, NY, 2008.

[35] Plimpton, S. J.; Pollock, R.; Stevens, M. In Particle-Mesh Ewald and Rrespa for Parallel Molecular Dynamics Simulations, the Eighth SIAM Conference on Parallel Processing for Scientific Computing, Minneapolis, 1997.

[36] Hockney, R. W.; Eastwood, J. W. Computer Simulation Using Particles; McGraw-Hill International Book Co.: New York, 1981.

[37] Plimpton, S. J. Fast Parallel Algorithms for Short-Range Molecular Dynamics. J. Comp. Phys. 1995, 117, 1−19.

[38] Swope, W. C.; Andersen, H. C.; Berens, P. H.; Wilson, K. R. A Computer-Simulation Method for the Calculation of Equilibrium- Constants for the Formation of Physical Clusters of Molecules - Application to Small Water Clusters. J. Chem. Phys. 1982, 76, 637− 649.

[39] Verlet, L. Phys. Rev. 1967, 159, 98.

[40] Nose, S. A Unified Formulation of the Constant Temperature Molecular- Dynamics Methods. J. Chem. Phys. 1984, 81, 511−519.

[41] Hoover, W. G. Canonical Dynamics - Equilibrium Phase-Space Distributions. Phys. Rev. A 1985, 31, 1695−1697.

[42] Cerius2 Modeling Environment, Release 4.0; Accelrys Inc.: San Diego, 1999.